MACROSCOPIC QUANTUM SUPERPOSITION IN A THREE-JOSEPHSON-JUNCTION LOOP

Caspar H. van der Wal[1], A. C. J. ter Haar[1], F. K. Wilhelm[1], R. N. Schouten[1], C. J. P. M. Harmans[1], T. P. Orlando[2], Seth Lloyd[3], J. E. Mooij[1,2]

[1] *Department of Applied Physics and*
Delft Institute for Micro Electronics and Submicron Technology (DIMES)
Delft University of Technology, P. O. Box 5046, 2600 GA Delft, the Netherlands
[2] *Department of Electrical Engineering and Computer Science and*
[3] *Department of Mechanical Engineering, MIT, Cambridge, MA 02139, USA*
Corresponding author, e-mail: caspar@qt.tn.tudelft.nl

Submitted for the proceedings of the MQC^2 workshop, Naples, June 14-17, 2000.

Abstract We present microwave-spectroscopy experiments on two quantum levels of a superconducting loop with three Josephson junctions. The level separation between the ground state and first excited state shows an anti-crossing where two classical persistent-current states with opposite polarity are degenerate. This is evidence for symmetric and anti-symmetric quantum superpositions of two macroscopic states; the classical states have persistent currents of 0.5 μA and correspond to the center-of-mass motion of millions of Cooper pairs. A study of the thermal occupancies of the two quantum levels shows that the loop is at low temperatures in a non-equilibrium state.

1. INTRODUCTION

A Josephson supercurrent is a macroscopic degree of freedom in the sense that it corresponds to the center-of-mass motion of a condensate with a very large number of Cooper pairs [1]. Even though the Josephson effect itself (with classical current and voltage variables) is often called a macroscopic quantum phenomena, Anderson [1], Leggett [2] and Likharev [3] discussed that a quantum superposition of Josephson currents would be a "true" [3] manifestation of quantum mechanics at a macroscopic scale. A simple system in which such a superposition can be studied is a superconducting loop containing one or more Josephson

tunnel junctions, where an external magnetic field is used to induce a persistent current in the loop. When the enclosed magnetic flux is close to half a superconducting flux quantum Φ_0, the loop may have multiple stable persistent-current states. The weak coupling of the Josephson junctions then allows for transitions between the states. At very low temperatures, the persistent-current states are very well decoupled from environmental degrees of freedom; excitations of individual charge carriers around the center of mass of the Cooper-pair condensate are prohibited by the superconducting gap. As a result, the transitions between the states can be a quantum coherent process, and superpositions of the macroscopic persistent-current states should be possible (loss of quantum coherence results from coupling to an environment with many degrees of freedom [4]). Josephson junction loops therefore rank among the best systems for experimental tests of the validity of quantum mechanics for systems containing a macroscopic number of particles [2, 5]. The potential for quantum coherent dynamics has stimulated research aimed at applying Josephson junction loops as basic building blocks for quantum computation (qubits) [6, 7, 8, 9].

We report in this chapter on microwave-spectroscopy experiments that demonstrate quantum superpositions of two macroscopic persistent-current states in a small loop with three Josephson junctions (Fig. 1, this is the qubit system discussed in [8, 9]). At an applied magnetic flux of $\frac{1}{2}\Phi_0$ this system behaves as a particle in a double-well potential, where the classical states in each well correspond to persistent currents of opposite sign (Fig. 1c). The two classical states are coupled via quantum tunneling through the barrier between the wells, and the loop is a macroscopic quantum two-level system. The energy levels vary with the applied flux as shown. While classically the levels should cross at $\frac{1}{2}\Phi_0$, quantum tunneling leads to an avoided crossing with symmetric and anti-symmetric superpositions of the two macroscopic persistent-current states. An inductively coupled DC-SQUID magnetometer was used to measure the flux generated by the loop's persistent current, while at the same time low-amplitude microwaves were applied to induce transitions between the levels (Fig. 2). We observed narrow resonance lines at magnetic field values where the level separation ΔE was resonant with the microwave frequency. The level separation shows the expected anti-crossing at $\frac{1}{2}\Phi_0$ (Fig. 3), which is interpreted as evidence for macroscopic superposition states [10, 11]. A study of the thermal broadening of the transition between the two states at $\frac{1}{2}\Phi_0$ shows that the loop is at low temperatures in a non-equilibrium state (Fig. 4).

Note that we have a scheme in which the meter (the DC-SQUID) is performing a measurement on a single quantum system. We should

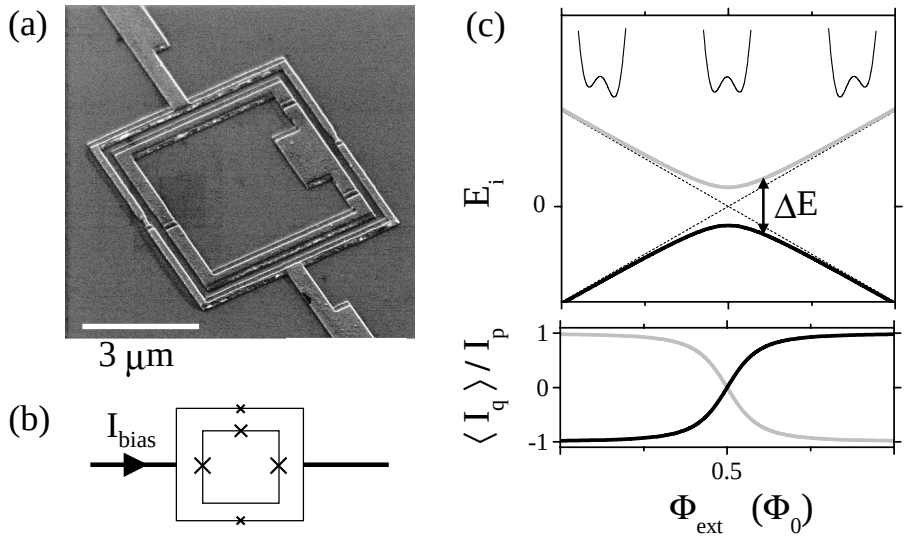

Figure 1 SEM-image (a) and schematic (b) of the small superconducting loop with three Josephson junctions (denoted by the crosses). The loop is inductively coupled to an underdamped DC-SQUID which is positioned around the loop. (c) Energy levels and persistent currents of the loop as a function of applied flux $\Phi_{\rm ext}$. The insets of the top plot show the double-well potential that is formed by the loop's total Josephson energy, plotted for a $\Phi_{\rm ext}$-value below $\frac{1}{2}\Phi_0$ (left), at $\frac{1}{2}\Phi_0$ (middle), and above $\frac{1}{2}\Phi_0$ (right). The horizontal axis for these potentials is a Josephson phase coordinate. The loop's two classical persistent-current states are degenerate at $\Phi_{\rm ext} = \frac{1}{2}\Phi_0$ (dashed lines). The quantum levels (solid lines) show level repulsion at this point, and are separated in energy by ΔE. The bottom plot shows the quantum mechanical expectation value $\langle I_{\rm q}\rangle = -\partial E_{\rm i}/\partial\Phi_{\rm ext}$ of the persistent current in the loop, for the ground state (black) and the excited state (grey), plotted in units of $I_{\rm p}$.

therefore expect that the measuring process is limiting the coherence of our system. While the system is pumped by the microwaves, the SQUID is actively measuring the flux produced by the persistent currents of the two states. Detecting the quantum levels of the loop is still possible since the meter is only weakly coupled to the loop. The flux signal needs to be built up by averaging over many repeated measurements on the same system, such that effectively an ensemble average is determined (time-ensemble). We measure the level separation, i. e. energy, rather than flux, since we perform spectroscopy; we observe a shift in averaged flux when the microwaves are resonant with the level separation. In our experiment we also chose to work with an extremely underdamped DC-

SQUID with unshunted junctions to minimize damping of the quantum system via the inductive coupling to the SQUID.

A recent paper by Friedman *et al.* [12] reports on similar results obtained from spectroscopy on excited states in a loop with a single junction (RF-SQUID). Previous experiments on RF-SQUIDs have demonstrated resonant tunneling between discrete quantum states in two wells [13, 14] and microwave-induced transitions between the wells [15]. Other observations that have been related to macroscopic superposition states are tunnel splittings observed with magnetic molecular clusters [16] and quantum interference of C_{60} molecules [17]. In quantum dots [18] and superconducting circuits where charge effects dominate over the Josephson effect [19, 20, 21] superpositions of charge states have been observed, as well as quantum coherent charge oscillations [22].

A quantum description of our system was reported in Refs. [8, 9]. It is a low-inductance loop intersected by three extremely underdamped Josephson junctions (Fig. 1), which are characterized by their Josephson coupling $E_{\rm J}$ and charging energy $E_{\rm C} = e^2/2C$. Here C is the junction capacitance and e the electron charge. The critical current of a junction is $I_{\rm C0} = \frac{2e}{\hbar}E_{\rm J}$, where $\hbar = \frac{h}{2\pi}$ is Planck's reduced constant. One of the junctions in the loop has $E_{\rm J}$ and C smaller by a factor $\beta \approx 0.8$. At an applied flux $\Phi_{\rm ext}$ close to $\frac{1}{2}\Phi_0$ the total Josephson energy forms a double well potential. The classical states at the bottom of each well have persistent currents of opposite sign, with a magnitude $I_{\rm p}$ very close to $I_{\rm C0}$ of the weakest junction, and with energies $E = \pm I_{\rm p}(\Phi_{\rm ext} - \frac{1}{2}\Phi_0)$ (dashed lines in Fig. 1c). We assume here $\Phi_{\rm ext}$ to be the total flux in the loop (the small self-generated flux due to the persistent currents leads to a constant lowering of the energies, but the crossing remains at $\frac{1}{2}\Phi_0$). The system can be pictured as a particle with a mass proportional to C in the Josephson potential; the electrostatic energy is the particle's kinetic energy. The charging effects are conjugate to the Josephson effect. For low-capacitance junctions (small mass) quantum tunneling of the particle through the barrier gives a tunnel coupling t between the persistent-current states. In the presence of quantum tunneling and for $E_{\rm J}/E_{\rm C}$-values between 10 and 100, the system should have two low-energy quantum levels E_0 and E_1, which can be described using a simple quantum two-level picture [8, 9], $E_{0(1)} = -(+)\sqrt{t^2 + \left(I_{\rm p}(\Phi_{\rm ext} - \frac{1}{2}\Phi_0)\right)^2}$. The loop's level separation $\Delta E = E_1 - E_0$ is then

$$\Delta E = \sqrt{(2t)^2 + \left(2I_{\rm p}(\Phi_{\rm ext} - \frac{1}{2}\Phi_0)\right)^2}. \qquad (1.1)$$

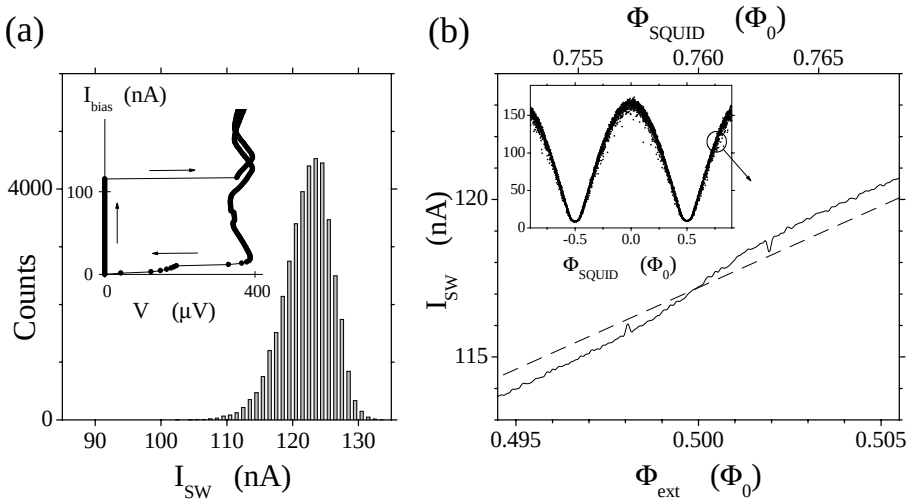

Figure 2 (a) Current-voltage characteristic (inset) and switching-current histogram of the underdamped DC-SQUID. The $I_{\rm bias}$-level where the SQUID switches from the supercurrent branch to a finite voltage state –the switching current $I_{\rm SW}$– is a measure for the flux in the loop of the DC-SQUID. The histogram in the main plot shows that the variance in $I_{\rm SW}$ is much larger than the flux signal of the inner loop's persistent current, which gives a shift in $I_{\rm SW}$ of about 1 nA. (b) The inset shows the modulation of $I_{\rm SW}$ versus the flux $\Phi_{\rm SQUID}$ applied to the DC-SQUID loop (data not averaged, one point per switching event). The main figure shows the averaged level of $I_{\rm SW}$ (solid line) near $\Phi_{\rm SQUID} = 0.76\,\Phi_0$. At this point the flux in the inner loop $\Phi_{\rm ext} \approx \frac{1}{2}\Phi_0$. The rounded step at $\Phi_{\rm ext} = \frac{1}{2}\Phi_0$ indicates the change of sign in the persistent current of the loop's ground state. In the presence of continuous-wave microwaves (here 5.895 GHz) a peak and a dip appear in the signal, symmetrically around $\frac{1}{2}\Phi_0$. The background signal of the DC-SQUID that results from flux directly applied to its loop (dashed line) is subtracted from the data presented in Figs. 3a and 4a.

2. EXPERIMENTAL REALIZATION

The system was realized by microfabricating an aluminum micrometer-sized loop with unshunted Josephson junctions (Fig. 1a). The sample consisted of a 5 x 5 μm^2 aluminum loop with aluminum-oxide tunnel junctions, microfabricated with e-beam lithography and shadow-evaporation techniques on a SiO_2 substrate. The electrodes of the loop were 450 nm wide and 80 nm thick. The DC-SQUID magnetometer was fabricated in the same layer around the inner loop, with a 7 x 7 μm^2 loop and smaller Josephson junctions that were as underdamped as the junctions of the inner loop. The DC-SQUID had an on-chip superconducting shunt capacitance of 2 pF and superconducting leads in four-point con-

figuration. The sample was mounted in a dilution refrigerator, inside a microwave-tight copper measurement box, magnetically shielded by two mu-metal and one superconducting shield. All spectroscopy measurements were taken with the temperature stabilized at 30 ± 0.05 mK. Microwaves were applied to the sample by a coaxial line, which was shorted at the end by a small loop of 5 mm diameter. This loop was positioned parallel to the sample plane at about 1 mm distance. Switching currents were measured with dedicated electronics, with repetition rates up to 9 kHz and bias currents ramped at typically 1 μA/ms (further details of the fabrication and experimental techniques can be found in Ref. [23]). Loop parameters estimated from test junctions fabricated on the same chip and electron-microscope inspection of the measured device give $I_{\rm p} = 450 \pm 50$ nA, $\beta = 0.82 \pm 0.1$, $C = 2.6 \pm 0.4$ fF for the largest junctions in the loop, giving $E_{\rm J}/E_{\rm C} = 38 \pm 8$. Due to the exponential dependence of the tunnel coupling t on the mass (C) and the size of the tunnel barrier, these parameters allow for a value for t/h between 0.2 and 5 GHz. The parameters of the DC-SQUID junctions were $I_{\rm C0} = 109 \pm 5$ nA and $C = 0.6 \pm 0.1$ fF. The self inductance of the inner loop and the DC-SQUID loop were numerically estimated to be 11 ± 1 pH and 16 ± 1 pH respectively, and the mutual inductance between the loop and the SQUID was 7 ± 1 pH.

The flux in the DC-SQUID was measured by ramping a bias current through the DC-SQUID and recording the current level $I_{\rm SW}$ where the SQUID switches from the supercurrent branch to a finite voltage (Fig. 2a). Traces of the loop's flux signal were recorded by continuously repeating switching-current measurements while slowly sweeping the flux $\Phi_{\rm ext}$ (Fig. 2b). The measured flux signal from the inner loop will be presented as $\tilde{I}_{\rm SW}$, which is directly deduced from the raw switching-current data, as described in the following three points:
1) Because the variance in $I_{\rm SW}$ was much larger than the signature from the loop's flux (Fig. 2a) we applied low-pass FFT-filtering in $\Phi_{\rm ext}$-space (over 10^7 switching events for the highest trace, and $2 \cdot 10^8$ events for the lowest trace in Fig. 3a).
2) By applying $\Phi_{\rm ext}$ we also apply flux directly to the DC-SQUID. The resulting background signal (dashed line in Fig. 2b) was subtracted.
3) Applying microwaves and changing the sample temperature influenced the switching current levels significantly. To make the flux signal of all data sets comparable we scaled all data sets to $I_{\rm SW} = 100$ nA at $\Phi_{\rm ext} = \frac{1}{2}\Phi_0$. Data taken in the presence of microwaves could only be obtained at specific frequencies where $I_{\rm SW}$ was not strongly suppressed by the microwaves. At temperatures above 300 mK drift in the $I_{\rm SW}$-level due to thermal instabilities of the refrigerator obscured the signal.

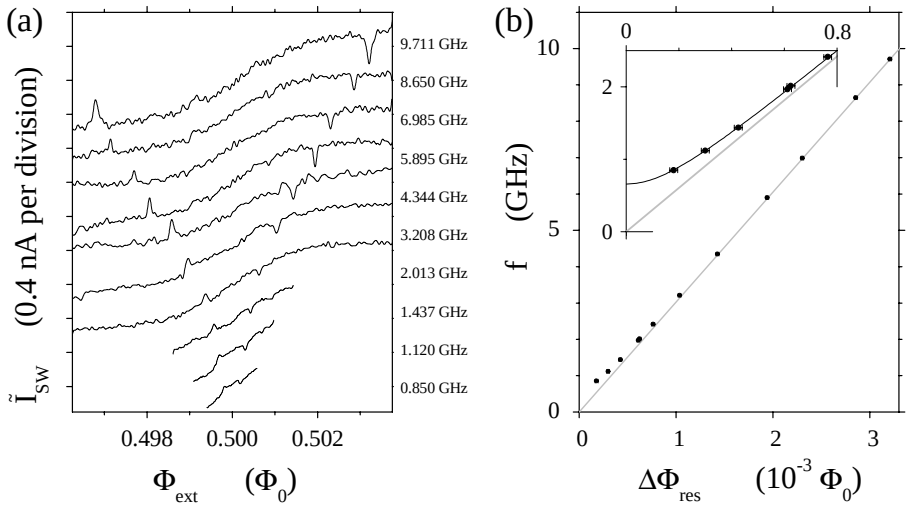

Figure 3 (a) Resonance lines in traces of the scaled switching current $\tilde{I}_{\rm SW}$ versus $\Phi_{\rm ext}$, measured at different microwave frequencies f (labels on the right). (b) Half the distance in $\Phi_{\rm ext}$ between the resonant peak and dip $\Delta\Phi_{\rm res}$ at different microwave frequencies f. Peak and dip positions are determined from traces as in Fig. 3a. The inset zooms in on the low frequency data points. The grey line is a linear fit through the high frequency data and zero. The black line is a fit of (1).

3. RESULTS

Figs. 2b and 3a show the flux signal of the inner loop, measured in the presence of low-amplitude continuous-wave microwaves at different frequencies f. The rounded step in each trace at $\frac{1}{2}\Phi_0$ is due to the change in direction of the persistent current of the loop's ground state (see also Fig. 1c). Symmetrically around $\Phi_{\rm ext} = \frac{1}{2}\Phi_0$ each trace shows a peak and a dip, which were absent when no microwaves were applied. The positions of the peaks and dips in $\Phi_{\rm ext}$ depend on microwave frequency but not on amplitude. The peaks and dips result from microwave-induced transitions to the state with a persistent current of opposite sign. These occur when the level separation is resonant with the microwave frequency, $\Delta E = hf$.

In Fig. 3b half the distance in $\Phi_{\rm ext}$ between the resonant peak and dip $\Delta\Phi_{\rm res}$ is plotted for all the frequencies f. The relation between ΔE and $\Phi_{\rm ext}$ is linear for the high-frequency data. This gives $I_{\rm p} = 484 \pm 2$ nA, in good agreement with the predicted value. At lower frequencies $\Delta\Phi_{\rm res}$ significantly deviates from this linear relation, demonstrating the

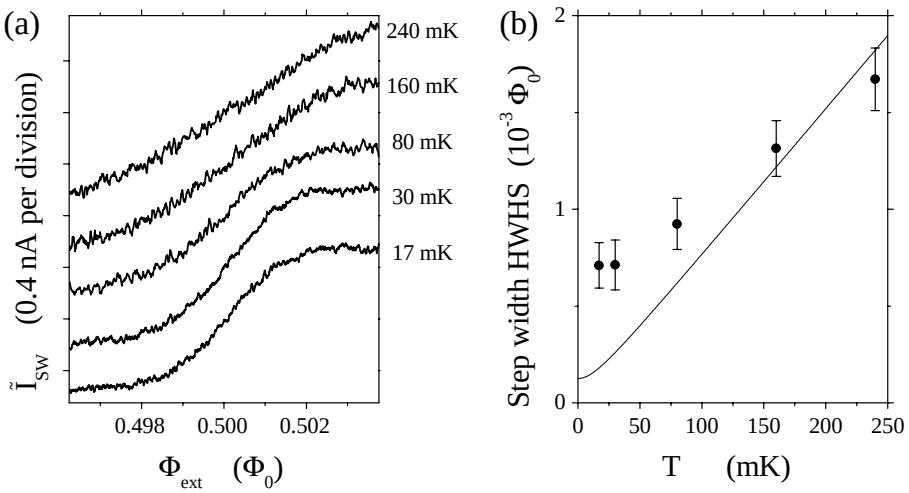

Figure 4 (a) $\tilde{I}_{\rm SW}$ versus $\Phi_{\rm ext}$, measured at different temperatures T (labels on the right). No microwaves were applied. The step in $\tilde{I}_{\rm SW}$ broadens with temperature. (b) The width of the step as a function of temperature. The half-width-half-step (HWHS) is defined as the distance in $\Phi_{\rm ext}$ from $\frac{1}{2}\Phi_0$ to the point where the amplitude of the step is half completed. The solid line is the calculated HWHS for thermally mixed levels, using (1) and the $I_{\rm p}$ and t-value from the spectroscopy results, with a saturating width on the scale of t at low temperatures.

presence of a finite tunnel splitting at $\Phi_{\rm ext} = \frac{1}{2}\Phi_0$. A fit to Eq. (1) yields $t/h = 0.33 \pm 0.03$ GHz, in agreement with the estimate from fabrication parameters. The level separation very close to $\frac{1}{2}\Phi_0$ could not be measured directly since at this point the expectation value for the persistent current is zero for both the ground state and the excited state (Fig. 1c). Nevertheless, the narrow resonance lines allow for an accurate mapping of the level separation near $\frac{1}{2}\Phi_0$, and the observed tunnel splitting gives clear evidence for quantum superpositions of the persistent-current states. The large uncertainty in the predicted t-value does not allow for a quantitative analysis of a possible suppression of t due to a coupling between our two-level system and a bosonic environment [24] or a spin-bath environment [25, 26]. However, the fact that we see a finite tunnel splitting indicates that the damping of our quantum system by environmental degrees of freedom is weak. The dimensionless dissipation parameter α introduced by Leggett *et al.* [24] must be $\alpha < 1$.

The width of the rounded steps in the measured flux in Figs. 2b and 3a is much broader than expected from quantum rounding on the scale

of the value of t that was found with spectroscopy (see also Fig. 1c). The temperature dependence of the step width presented in Fig. 4 confirms that the step width HWHS (defined in the caption of Fig. 4b) is too wide at low temperatures T. At temperatures above 100 mK the step width is in agreement with the thermally averaged expectation value for the persistent current $< I_{\rm th} >= I_{\rm p} \tanh\left(\frac{\Delta E}{2k_{\rm B}T}\right)$ ($k_{\rm B}$ is Boltzmann's constant), where we use the level separation ΔE and $I_{\rm p}$ found with spectroscopy. However, when lowering the temperature the observed step width saturates at an effective temperature of about 100 mK. We checked that the effective temperature for the SQUID's switching events did not saturate at the lowest temperatures. The high effective temperature of the loop is a result of the loop being in a non-equilibrium state. Cooling the sample longer after the dissipative switching events did not make the step narrower. The step width at $T = 30$ mK was measured with 100 μs and 50 ms dead time between switching events, but no significant differences were found. This indicates that the out-of-equilibrium population of the excited state is caused by the measurement process with the SQUID or other weakly coupled external processes, in combination with a long time scale for cooling the system to equilibrium (as can be expected since it is very well isolated from the environment). Note that the observed line width and the level separation near $\frac{1}{2}\Phi_0$ are small compared to the effective temperature of 100 mK. Silvestrini *et al.* [27] showed that this can be the case in a Josephson junction system when the transitions between the levels occur much faster than the thermal mixing time, a phenomena that is also well known from e. g. room-temperature NMR on liquids.

4. CONCLUSION

We have presented clear evidence that a quantum superposition of two macroscopic persistent currents can occur in a small Josephson junction loop. Even though the measuring DC-SQUID is contributing significantly to the decoherence of our system (see also Ref. [11]), it was possible to detect the superposition states since the SQUID was only weakly coupled to the loop. The present results demonstrate the potential of three-junction persistent-current loops for research on macroscopic quantum coherence and quantum computation.

Acknowledgments

We thank J. B. Majer, A. C. Wallast, L. Tian, D. S. Crankshaw, J. Schmidt, A. Wallraff and L. Levitov for help and stimulating discussions. This work was financially supported by the Dutch Foundation for Fundamental Research on Matter

(FOM), the European TMR research network on superconducting nanocircuits (SUPNAN), the USA Army Research Office (grant DAAG55-98-1-0369) and the NEDO joint research program (NTDP-98).

References

[1] P. W. Anderson, in *Lectures on the Many-Body Problem*, E. R. Caianiello, Ed. (Academic Press, New York, 1964), vol. 2, pp. 113-135.

[2] A. J. Leggett, *Prog. Theor. Phys. Suppl.* **69**, 80 (1980).

[3] K. K. Likharev, *Sov. Phys. Usp.* **26**, 87 (1983).

[4] W. H. Zurek, *Phys. Today* **44**, 36 (October 1991).

[5] A. J. Leggett, A. Garg, *Phys. Rev. Lett.* **54**, 857 (1985).

[6] M. F. Bocko *et al.*, *IEEE Trans. Appl. Supercond.* **7**, 3638 (1997).

[7] L. B. Ioffe *et al.*, *Nature* **398**, 679 (1999).

[8] J. E. Mooij *et al.*, *Science* **285**, 1036 (1999).

[9] T. P. Orlando *et al.*, *Phys. Rev. B.* **60**, 15398 (1999).

[10] We acknowledge that the results presented here do not exclude alternative theories for quantum mechanics (e. g. macro-realistic theories). This would require a type of experiment as proposed by Leggett *et al.* [5].

[11] C. H. van der Wal *et al.*, submitted to *Science*.

[12] J. R. Friedman *et al.*, *Nature* **406**, 43 (2000).

[13] R. Rouse, S. Han, J. E. Lukens, *Phys. Rev. Lett.* **75**, 1614 (1995).

[14] C. Cosmelli *et al.*, *Phys. Rev. Lett.* **82**, 5357 (1999).

[15] S. Han, R. Rouse, J. E. Lukens, *Phys. Rev. Lett.* **84**, 1300 (2000).

[16] W. Wernsdorfer, R. Sessoli, *Science* **284**, 133 (1999).

[17] M. Arndt *et al.*, *Nature* **401**, 680 (1999).

[18] T. H. Oosterkamp *et al.*, *Nature* **395**, 873 (1998).

[19] Y. Nakamura *et al.*, *Phys. Rev. Lett.* **79**, 2328 (1997).

[20] V. Bouchiat *et al.*, *Phys. Scr.* **T76**, 165 (1998).

[21] D. J. Flees, S. Han, J. E. Lukens, *J. Supercond.* **12**, 813 (1999).

[22] Y. Nakamura, Yu. A. Pashkin, J. S. Tsai, *Nature* **398**, 786 (1999).

[23] C. H. van der Wal, J. E. Mooij, *J. Supercond.* **12**, 807 (1999).

[24] A. J. Leggett *et al.*, *Rev. Mod. Phys.* **59**, 1 (1987).

[25] N. Prokof'ev, P. Stamp, *Rep. Prog. Phys.* **63**, 669 (2000).

[26] L. Tian *et al.*, to be published; cond-mat/9910062.

[27] P. Silvestrini *et al.*, *Phys. Rev. Lett.* **79**, 3046 (1997).